2014 IEEE/RSJ International Conference on
Intelligent Robots and Systems (IROS 2014)
September 14-18, 2014, Chicago, IL, USA

Towards Simultaneous Coordinate Calibrations for Cooperative Multiple Robots

Jiaole Wang[1,2,†], Liao Wu[2,†], Max Q.-H. Meng[1], *Fellow, IEEE*, and Hongliang Ren[2,*], *Member, IEEE*

***Abstract*— Tasks that are too hard for single robot can be easily carried out by multiple robots in a cooperative manner. If some/all robots have mobile bases, the cooperation is subjected to great uncertainties in both the robotic system and environment. Therefore, the relationships among all the base frames (robot-robot calibration) and the relationships between the end-effectors and the other devices such as cameras and tools (hand-eye and tool-flange calibrations) have to be calculated to enable the robots to cooperate. To address these challenges, in this paper, we propose a simultaneous hand-eye, tool-flange and robot-robot calibration method. Thorough simulations are conducted to show the superiority of the proposed simultaneous method under different noise levels and various numbers of robot movements. Furthermore, the comparison to two non-simultaneous calibration methods has also been carried out to show the efficiency and robustness of the proposed simultaneous method.**

***Index Terms*— Multiple robot cooperation; Hand-eye calibration; Tool-flange calibration; Robot-robot calibration; AXB = YCZ problem**

I. INTRODUCTION

When multiple robots work in a cooperative manner, tasks that are considered to be too complicated or even impossible for single robot will be easily handled. Multi-robot cooperation opens new possibilities to accomplish tasks in many circumstances including new applications of robotics in surgical procedures, space, underwater, construction, etc. [1]–[5].

Robot cooperation can be roughly classified into two kinds of setups: static and dynamic setups. For the static setup, all the bases of the involved robots are immobile and the robotic system is in a relatively static environment. Therefore, the relationships among all the base frames (robot-robot calibration) are invariant, which can be defined by mechanical design accurately. This static setup also makes the calculation easier for the relationships between the end-effectors and the other devices such as cameras and tools (hand-eye and tool-flange calibrations). For the dynamic setup, such as a setup comprising multiple mobile manipulators [1], [2], great uncertainties exist in both the robotic system and environment, because of the mobility of the bases of all/some robots. For the cooperative task that needs high accuracy, such as cooperative robotic surgery by multiple robots [4]–[9] or navigated minimally invasive surgeries guided by multiple sensing modalities [10]–[16], coordinate calibration must be done first to ensure expected performance.

On one hand, the mobility of the robot base makes robotic cooperation impossible without calibrating the robot-to-robot relationships. On the other hand, it is important for the robots to be able to change tools and/or sensors in order to handle different situations in the practical scenario. Thus, hand-eye and tool-flange relationships are definitely needed. Consequently, the hand-eye, tool-flange and robot-robot relationships have to be determined frequently in order to enable the robots to cooperate inside the constantly changing environment.

A. Related Work

In order to utilize a hand-mounted sensor (such as a camera, a range-finder, etc.) to carry out precise manipulation, hand-eye calibration [17], [18] has been the first problem that the robotic system has to solve. The hand-eye calibration problem can be formulated by a matrix equation as $\mathbf{AX} = \mathbf{XB}$, where $\mathbf{A}, \mathbf{B}$ are the homogeneous transformation matrices of end-effector and camera movements, respectively. And $\mathbf{X}$ is the unknown relationship between the robotic hand and the sensor. Then at least two relative motions with non-parallel rotational axes are needed to solve the unknown $\mathbf{X}$ [17], [19]. This calibration problem has been thoroughly studied and many methods have been proposed [20]–[24].

As an extension of the hand-eye calibration, the robot-world and hand-eye calibration defines a problem that the relationship between the world frame and the robot base frame is also unknown [25], [26]. This problem could be expressed by a homogeneous transformation equation $\mathbf{AX} = \mathbf{YB}$, where $\mathbf{Y}$ is the robot to world rigid transformation. Similarly, this robot-world and hand-eye calibration problem can be solved provided two relative motions with non-parallel rotational axes [25]. This problem has been well studied by [27]–[29].

Along with the rapid development of unmanned aerial vehicle (UAV), robot-robot calibration has become a prerequisite for the multiple UAV cooperation [30]. In order to carry out tasks cooperatively, the relative robot-robot translation and rotation must be calculated frequently. Zhou et al. [31], [32] summarized that robot-robot homogeneous transformation has 14 base minimal situations by considering all possible combinations of inter-robot measurements. The closed-form and analytic solutions have been given except for two singular situations.

[1]Jiaole Wang and Max Q.-H. Meng are with the Department of Electronic Engineering, The Chinese University of Hong Kong, N.T., Hong Kong SAR, China jlwang@ee.cuhk.edu.hk, max@ee.cuhk.edu.hk

[2]Jiaole Wang, Liao Wu, and Hongliang Ren are with the Department of Biomedical Engineering, National University of Singapore, Singapore biewul@nus.edu.sg/wuliaothu@gmail.com, ren@nus.edu.sg

[†]These authors contributed equally.

[*]Corresponding author.

B. The Proposed Methods and Original Contributions

In this paper, we propose one simultaneous calibration method to solve the hand-eye, tool-flange and robot-robot calibration problem for the tasks which need to be done by cooperative multiple robot.

The contributions of our work are summarized as follows:

- A fundamental calibration problem for the practice of multiple robot cooperation is modeled and formulated as an $\mathbf{AXB} = \mathbf{YCZ}$ problem for the first time (to the best of our knowledge).
- An efficient iterative solution is presented to simultaneously solve the problem.
- A comparison between the simultaneous method and the non-simultaneous ones are carried out to show the efficiency and robustness of the proposed simultaneous method.

The rest of the paper is organized as follows: Section II models and formulates the calibration problem, followed by the proposed solutions, mathematical interpretations and algorithms. The simulation results, including algorithm comparison and other analysis, are illustrated in Section III. We further discuss the results and the gained insights in Section IV, and draw some conclusions at the end of this paper.

II. METHODS

Without loss of generality, we assume a scenario with two arbitrary manipulator mounted mobile robots as shown in the Fig. 1. The homogeneous transformations of the two robot end-effector frames with respect to their base frames are denoted as the measurable data $\mathbf{A}_i$ and $\mathbf{C}_i$, where i stands for the ith measurement. We here made an assumption that all the manipulators are well calibrated and the kinematic parameters are known.

The homogeneous transformation of the tool held by one robot hand with respect to the sensor ("eye") held by the other is denoted as $\mathbf{B}_i$, which is also a measurable data that can be obtained by using a sensor (such as optical tracker, camera, etc.) and a marker (such as LED, reflecting balls, fiducial pattern, etc.). Then, the three unknowns are defined as the homogeneous transformations from one robot base frame to another ($\mathbf{Y}$), from eye/tool to hand/flange ($\mathbf{X}$ and $\mathbf{Z}$). A transformation loop can be formed by the measurable data $\mathbf{A}$, $\mathbf{B}$ and $\mathbf{C}$, and the unknowns $\mathbf{X}$, $\mathbf{Y}$ and $\mathbf{Z}$ as the following equation,

$$\mathbf{AXB} = \mathbf{YCZ}. \tag{1}$$

Intuitively, a 3-step method can be employed to solve $\mathbf{X}$, $\mathbf{Z}$ and $\mathbf{Y}$ sequentially. The $\mathbf{X}$ and $\mathbf{Z}$ in (1) can be separately calculated as two hand-eye/tool-flange calibrations through $\mathbf{AX} = \mathbf{XB}$ problem and the last unknown robot-robot relationship $\mathbf{Y}$ can be solved directly using the previously retrieved data by the method of least squares.

Alternatively, the latter two steps of solving $\mathbf{Z}$ and $\mathbf{Y}$ of the above approach can be expressed as $(\mathbf{AXB})\mathbf{Z}^{-1} = \mathbf{YC}$, which can be treated and solved simultaneously as an $\mathbf{AX} = \mathbf{YB}$ problem [27]–[29]. This is referred as the 2-step method.

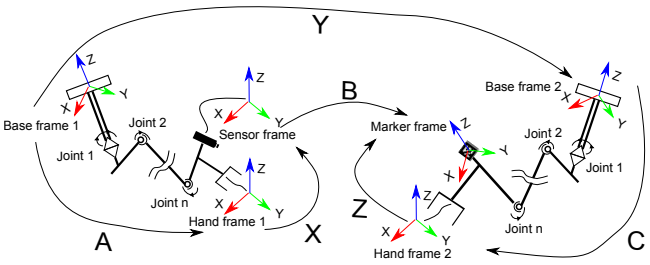

Fig. 1. The hand-eye, tool-flange and robot-robot calibration problem which can be formulated in a matrix equation as $AXB = YCZ$.

Both 2-step method and 3-Step method need at least 6 sets of data, i.e. data sets ($\mathbf{A}_{1,2,3}$, $\mathbf{B}_{1,2,3}$) in the first data acquisition procedure and ($\mathbf{C}_{1,2,3}$, $\mathbf{B}_{4,5,6}$) in the second or third step.

The simultaneous method proposed in this paper shortens data acquisition procedures in the non-simultaneous methods and needs only at least 3 sets of appropriate data to solve the original **AXB = YCZ** equation. During the data acquisition procedure, two manipulators synchronously or asynchronously carry out at least two relative motions whose rotational axes are not parallel. The obtained data sets are ($\mathbf{A}_{1,2,3}$, $\mathbf{B}_{1,2,3}$, $\mathbf{C}_{1,2,3}$). The detailed algorithm and mathematical interpretations are introduced in Section II-A.

A. Algorithm Development

The rotational and translational components are separately solved for the three unknowns in the $\mathbf{AXB} = \mathbf{YCZ}$ equation. By expending the homogeneous transformation matrices, the following two equations can be derived:

$$\mathbf{R}_A\mathbf{R}_X\mathbf{R}_B = \mathbf{R}_Y\mathbf{R}_C\mathbf{R}_Z, \tag{2}$$

$$\mathbf{R}_A\mathbf{R}_X\mathbf{t}_B + \mathbf{R}_A\mathbf{t}_X + \mathbf{t}_A = \mathbf{R}_Y\mathbf{R}_C\mathbf{t}_Z + \mathbf{R}_Y\mathbf{t}_C + \mathbf{t}_Y, \tag{3}$$

where $\mathbf{R}$ is a 3×3 rotation matrix, and $\mathbf{t}$ is a 3×1 translation vector. We will first solve $\mathbf{R}_X, \mathbf{R}_Y, \mathbf{R}_Z$ from (2), and then find $\mathbf{t}_X, \mathbf{t}_Y, \mathbf{t}_Z$ from (3) using the solved rotation matrices.

1) Solution to the Rotational Components: As there is a coupling between $\mathbf{R}_Y$ and $\mathbf{R}_Z$, (2) evinces strong nonlinearity. As a result, it is difficult to find a closed-form solution to the rotation matrices. We put forward a linear approximation iterative method to solve the problem, which mainly uses the variation of rotation matrices.

Being an element of the Lie group $SO(3)$, a rotation matrix can be exponentially mapped by its Lie algebra $[\mathbf{r}]^\wedge$ as [33]

$$\mathbf{R} = \exp\left([\mathbf{r}]^\wedge\right) = \mathbf{I} + \frac{\sin(\|\mathbf{r}\|)}{\|\mathbf{r}\|}[\mathbf{r}]^\wedge + \frac{1-\cos(\|\mathbf{r}\|)}{\|\mathbf{r}\|^2}\left([\mathbf{r}]^\wedge\right)^2, \tag{4}$$

where $\|\mathbf{r}\|$ gives the norm of the vector $\mathbf{r} = \begin{bmatrix} r_1 & r_2 & r_3 \end{bmatrix}^T$, and $[\mathbf{r}]^\wedge$ is the screw matrix of $\mathbf{r}$.

Using the Taylor series expansion of the exponential map, we have

$$\mathbf{R} = \exp\left([\mathbf{r}]^\wedge\right) = \mathbf{I} + \sum_{n=1}^{\infty}\frac{\left([\mathbf{r}]^\wedge\right)^n}{n!}. \tag{5}$$

If $\mathbf{R}$ is in the neighborhood of the identity $\mathbf{I}$, we are allowed to take a first-order approximation and obtain

$$\mathbf{R} \approx \mathbf{I} + [\mathbf{r}]^\wedge. \tag{6}$$

To utilize this property in our problem solving, we need to pull the arbitrary rotation matrix back to the neighborhood of $\mathbf{I}$. In order to do this, we rewrite (2) as

$$\begin{aligned}&\mathbf{R}_A\left(\mathbf{R}_{X,true}\mathbf{R}_{X,init}^{-1}\right)\mathbf{R}_{X,init}\mathbf{R}_B\\&=\left(\mathbf{R}_{Y,true}\mathbf{R}_{Y,init}^{-1}\right)\mathbf{R}_{Y,init}\mathbf{R}_C\left(\mathbf{R}_{Z,true}\mathbf{R}_{Z,init}^{-1}\right)\mathbf{R}_{Z,init},\end{aligned}\quad(7)$$

where $\mathbf{R}_{true}$ represents the true value of the rotation matrix we are looking for, and $\mathbf{R}_{init}$ means an initial guess of the true rotation. If the initial guess is good enough, $\mathbf{R}_{true}\mathbf{R}_{init}^{-1}$ will lie in the neighborhood of $\mathbf{I}$. Then by substituting (6), (7) can be formulated as

$$\begin{aligned}&\mathbf{R}_A\left(\mathbf{I}+[\Delta\mathbf{r}_X]^\wedge\right)\mathbf{R}_{X,init}\mathbf{R}_B\\&=\left(\mathbf{I}+[\Delta\mathbf{r}_Y]^\wedge\right)\mathbf{R}_{Y,init}\mathbf{R}_C\left(\mathbf{I}+[\Delta\mathbf{r}_Z]^\wedge\right)\mathbf{R}_{Z,init},\end{aligned}\quad(8)$$

where $[\Delta\mathbf{r}]^\wedge$ is the associate Lie algebra of $\mathbf{R}_{true}\mathbf{R}_{init}^{-1}$. By rearranging (8) and ignoring the second-order small quantity $[\Delta\mathbf{r}_Y]^\wedge[\Delta\mathbf{r}_Z]^\wedge$, (8) becomes

$$\begin{aligned}&\mathbf{R}_A[\Delta\mathbf{r}_X]^\wedge\mathbf{R}_{X,init}\mathbf{R}_B-[\Delta\mathbf{r}_Y]^\wedge\mathbf{R}_{Y,init}\mathbf{R}_C\mathbf{R}_{Z,init}\\&-\mathbf{R}_{Y,init}\mathbf{R}_C[\Delta\mathbf{r}_Z]^\wedge\mathbf{R}_{Z,init}=-\mathbf{R}_A\mathbf{R}_{X,init}\mathbf{R}_B+\mathbf{R}_{Y,init}\mathbf{R}_C\mathbf{R}_{Z,init}.\end{aligned}\quad(9)$$

It can be verified that for any two 3×1 vectors $\mathbf{a}$ and $\mathbf{b}$, the following relationship holds:

$$[\mathbf{a}]^\wedge\mathbf{b}=\mathbf{a}\times\mathbf{b}=-\mathbf{b}\times\mathbf{a}=-[\mathbf{b}]^\wedge\mathbf{a}.\quad(10)$$

Hence, by rewriting (9) column by column and utilizing (10), (9) can be converted into the following form:

$$\mathbf{F}\Delta\mathbf{r}=\mathbf{q},\quad(11)$$

where

$$\Delta\mathbf{r}=\begin{bmatrix}\Delta\mathbf{r}_X^T & \Delta\mathbf{r}_Y^T & \Delta\mathbf{r}_Z^T\end{bmatrix}_{1\times9}^T\quad(12)$$

$$\mathbf{q}=\begin{bmatrix}(-\mathbf{R}_A\mathbf{R}_{X,init}\mathbf{R}_B+\mathbf{R}_{Y,init}\mathbf{R}_C\mathbf{R}_{Z,init})_1\\(-\mathbf{R}_A\mathbf{R}_{X,init}\mathbf{R}_B+\mathbf{R}_{Y,init}\mathbf{R}_C\mathbf{R}_{Z,init})_2\\(-\mathbf{R}_A\mathbf{R}_{X,init}\mathbf{R}_B+\mathbf{R}_{Y,init}\mathbf{R}_C\mathbf{R}_{Z,init})_3\end{bmatrix}_{9\times1}\quad(13)$$

and $\mathbf{F}$ is defined in (14), where $(\bullet)_i$ $(i=1,2,3)$ means to extract the ith column from the matrix in the bracket.

Now suppose m $(m\geq3)$ sets of measurements are performed, each of which can be formulated as an equation in the form of (11). Stacking these equations, we obtain

$$\tilde{\mathbf{F}}\Delta\mathbf{r}=\tilde{\mathbf{q}},\quad(15)$$

where

$$\tilde{\mathbf{F}}=\begin{bmatrix}\mathbf{F}_1^T & \mathbf{F}_2^T & \cdots & \mathbf{F}_m^T\end{bmatrix}_{9\times9m}^T\quad(16)$$

$$\tilde{\mathbf{q}}=\begin{bmatrix}\mathbf{q}_1^T & \mathbf{q}_2^T & \cdots & \mathbf{q}_m^T\end{bmatrix}_{1\times9m}^T.\quad(17)$$

Then $\Delta\mathbf{r}$ can be solved in a least-square sense by

$$\Delta\mathbf{r}=\left(\tilde{\mathbf{F}}^T\tilde{\mathbf{F}}\right)^{-1}\tilde{\mathbf{F}}^T\tilde{\mathbf{q}}.\quad(18)$$

The obtained $\Delta\mathbf{r}$ is then used to update $\mathbf{R}_{init}$ by

$$\mathbf{R}_{init}^{new}=\exp(\Delta\mathbf{r}_i)\,\mathbf{R}_{init}^{old},\quad(19)$$

where $\Delta\mathbf{r}_i$ $(i=X,Y,Z)$ represents the components of $\Delta\mathbf{r}$ associated with $\mathbf{X}$, $\mathbf{Y}$, $\mathbf{Z}$, respectively.

The process iterates until the norm of $\Delta\mathbf{r}$ falls below a predefined threshold, which means that the variable converges at least to local optimum. To ensure the global optimum is reached, a good initial guess of the rotation matrices $\mathbf{R}_X$, $\mathbf{R}_Y$, and $\mathbf{R}_Z$ is necessary. While $\mathbf{R}_Y$, the rotation between the bases of the two robots, is relatively hard to estimate in advance, $\mathbf{R}_X$, the rotation between hand/eye, and $\mathbf{R}_Z$, the rotation between tool/flange, are generally easy to evaluate provided their mechanical dimensions. Then the initial value of $\mathbf{R}_Y$ can be calculated using any single measurement data according to (2).

2) Solution to the Translational Components: The solution to the translational components is trivial when the rotational components are solved already. Rewrite (3) in the following form:

$$\mathbf{J}\mathbf{t}=\mathbf{p},\quad(20)$$

where

$$\mathbf{J}=\begin{bmatrix}\mathbf{R}_A & -\mathbf{I} & -\mathbf{R}_Y\mathbf{R}_C\end{bmatrix}_{3\times9},\quad(21)$$

$$\mathbf{t}=\begin{bmatrix}\mathbf{t}_X^T & \mathbf{t}_Y^T & \mathbf{t}_Z^T\end{bmatrix}_{1\times9}^T,\quad(22)$$

$$\mathbf{p}=-\mathbf{t}_A-\mathbf{R}_A\mathbf{R}_X\mathbf{R}_B+\mathbf{R}_Y\mathbf{t}_C.\quad(23)$$

With m groups of data measured, we can similarly concatenate them together and have

$$\tilde{\mathbf{J}}\mathbf{t}=\tilde{\mathbf{p}}\quad(24)$$

where

$$\tilde{\mathbf{J}}=\begin{bmatrix}\mathbf{J}_1^T & \mathbf{J}_2^T & \cdots & \mathbf{J}_m^T\end{bmatrix}_{9\times3m}^T\quad(25)$$

$$\tilde{\mathbf{p}}=\begin{bmatrix}\mathbf{p}_1^T & \mathbf{p}_2^T & \cdots & \mathbf{p}_m^T\end{bmatrix}_{1\times3m}^T.\quad(26)$$

Hence, $\mathbf{t}$ can be simply solved by

$$\mathbf{t}=\left(\tilde{\mathbf{J}}^T\tilde{\mathbf{J}}\right)^{-1}\tilde{\mathbf{J}}^T\tilde{\mathbf{p}}.\quad(27)$$

III. RESULTS

Intensive simulations of the proposed two kinds of methods have been carried out under different noise levels and by using different numbers of data sets. To simplify the simulation, two 6 degrees-of-freedom (DOFs) PUMA 560 manipulators that mounted onto two mobile bases are used to simulate the hand-eye, tool-flange and robot-robot calibration problem. The PUMA 560 kinematic parameters used in the simulation are from [34]. The rotational errors (err_{rot}) and translational errors (err_{trl}) are defined in the following equations,

$$\begin{aligned}err_{rot}&=\theta(\mathbf{R}_{i,est}\,\mathbf{R}_{i,true}^{-1}),\\err_{trl}&=\|\mathbf{t}_{i,est}-\mathbf{t}_{i,true}\|,\end{aligned}\quad(28)$$

where $\theta(\bullet)$ stands for the calculation of the rotational angle, $\bullet_{est}$ and $\bullet_{true}$ stand for estimated and true values of the rotation matrices $\mathbf{R}_i$ and translation vectors $\mathbf{t}_i$, and i stands for the unknowns $\mathbf{X}$, $\mathbf{Y}$ and $\mathbf{Z}$.

$$\mathbf{F} = \begin{bmatrix} -\mathbf{R}_A\left[\left(\mathbf{R}_{X,init}\mathbf{R}_B\right)_1\right]^\wedge & \left[\left(\mathbf{R}_{Y,init}\mathbf{R}_C\mathbf{R}_{Z,init}\right)_1\right]^\wedge & \mathbf{R}_{Y,init}\mathbf{R}_C\left[\left(\mathbf{R}_{Z,init}\right)_1\right]^\wedge \\ -\mathbf{R}_A\left[\left(\mathbf{R}_{X,init}\mathbf{R}_B\right)_2\right]^\wedge & \left[\left(\mathbf{R}_{Y,init}\mathbf{R}_C\mathbf{R}_{Z,init}\right)_2\right]^\wedge & \mathbf{R}_{Y,init}\mathbf{R}_C\left[\left(\mathbf{R}_{Z,init}\right)_2\right]^\wedge \\ -\mathbf{R}_A\left[\left(\mathbf{R}_{X,init}\mathbf{R}_B\right)_3\right]^\wedge & \left[\left(\mathbf{R}_{Y,init}\mathbf{R}_C\mathbf{R}_{Z,init}\right)_3\right]^\wedge & \mathbf{R}_{Y,init}\mathbf{R}_C\left[\left(\mathbf{R}_{Z,init}\right)_3\right]^\wedge \end{bmatrix}_{9\times 9} \tag{14}$$

TABLE I

NOISES OF THREE LEVELS THAT INJECTED INTO THE MEASURED DATA.

	High Noise Level	Medium Noise Level	Low Noise Level
Rotational Noise (degree)	$\theta(\mathbf{R_A}), \theta(\mathbf{R_C}) \sim \mathscr{U}(-0.1, 0.1)$ $\theta(\mathbf{R_B}) \sim \mathscr{U}(-0.2, 0.2)$	$\theta(\mathbf{R_A}), \theta(\mathbf{R_C}) \sim \mathscr{U}(-0.05, 0.05)$ $\theta(\mathbf{R_B}) \sim \mathscr{U}(-0.1, 0.1)$	$\theta(\mathbf{R_A}), \theta(\mathbf{R_C}) \sim \mathscr{U}(-0.01, 0.01)$ $\theta(\mathbf{R_B}) \sim \mathscr{U}(-0.02, 0.02)$
Translational Noise (mm)	$\|\mathbf{t_A}\|, \|\mathbf{t_C}\| \sim \mathscr{U}(-0.5, 0.5)$ $\|\mathbf{t_B}\| \sim \mathscr{U}(-1, 1)$	$\|\mathbf{t_A}\|, \|\mathbf{t_C}\| \sim \mathscr{U}(-0.25, 0.25)$ $\|\mathbf{t_B}\| \sim \mathscr{U}(-0.5, 0.5)$	$\|\mathbf{t_A}\|, \|\mathbf{t_C}\| \sim \mathscr{U}(-0.05, 0.05)$ $\|\mathbf{t_B}\| \sim \mathscr{U}(-0.1, 0.1)$

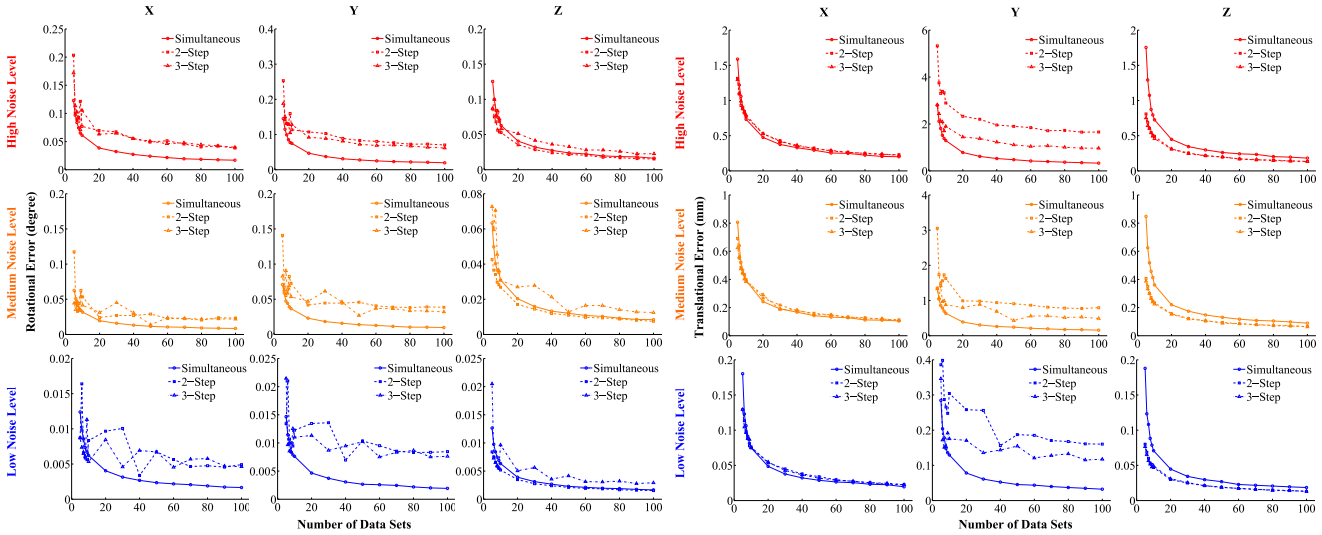

(a) Averaged rotational errors for three methods under three noise levels by using different numbers of data sets.

(b) Averaged translational errors for three methods under three noise levels by using different numbers of data sets.

Fig. 2. Averaged rotational and translational errors for three methods under three noise levels by using different numbers of data sets for solving hand-eye, tool-flange and robot-robot calibration ($\mathbf{AXB} = \mathbf{YCZ}$) problem. Red, orange and blue lines stand for high, medium and low noise level, respectively. The solid line with circle marker, the dash line with square marker, and the dash dot line with triangle marker denote the results of simultaneous, 2-Step and 3-Step methods, respectively.

A. *Influences of Noise and Number of Data Sets*

Synthetic noises which are uniformly distributed noises with different variances have been ejected to measurable matrices $\mathbf{A}_i$, $\mathbf{B}_i$ and $\mathbf{C}_i$. Because the measured data from hand-mounted sensors are more fragile to noises, $\mathbf{B}_i$ are corrupted by noises with greater variances. To investigate the effects of noise on the three proposed methods, three different kinds of noise levels which are listed in Table I have been injected to the measured data. It is noted that the rotational noises has been added to the angles $(\theta(\mathbf{R_A}), \theta(\mathbf{R_B}), \theta(\mathbf{R_C}))$, and the rotational axes are randomly generated. In addition, the translational noises has been added to the norms of the translation vectors $(\|\mathbf{t_A}\|, \|\mathbf{t_B}\|, \|\mathbf{t_C}\|)$ with random directions. The average errors of rotational and translational components of $\mathbf{X}, \mathbf{Y}, \mathbf{Z}$ under different noise levels over 500 random trials are shown in Fig. 2, where the red, orange and blue lines stand for high, medium and low noise level, respectively. It is clear that as the noise level decreases, the errors in both rotation and translation of all unknowns decrease.

Because the data acquisition process time and the final accuracy are all depended on data sets, we also investigate the influence of the number of data sets on the calibration. The averaged rotational and translational errors of $\mathbf{X}, \mathbf{Y}, \mathbf{Z}$ under $5, \cdots, 100$ sets of data are shown in Fig. 2. It is clearly shown that as the number of data sets increases, the errors in both rotation and translation decrease, however, the rotational errors in $\mathbf{X}, \mathbf{Y}, \mathbf{Z}$ show an acute descent around 10 while translation errors show a gradual change. A convergence could be observed around 60 in both errors.

B. *Simultaneous Method Versus Non-simultaneous Methods*

A comparison has been made based on various simulations of the simultaneous method and two non-simultaneous methods (3-Step and 2-Step methods) under different noise levels and numbers of data sets. Data used in the simulations are generated in different ways for these two kind of methods since they require different calibration processes as

introduced in Section II. For the 3-Step method, $\mathbf{X}$ and $\mathbf{Z}$ are first calculated in a hand-eye calibration manner by using the algorithms proposed by Tsai et al. [18]. For the 2-Step method, in which the first step is carried out in an $\mathbf{AX} = \mathbf{XB}$ manner, a robot-world and hand-eye calibration that solves $\mathbf{AX} = \mathbf{YB}$ problem is carried out by using the algorithms proposed by Li et al. [27].

The simulation results are shown in Fig. 2, where the solid line with circle marker, the dash line with square marker and the dash dot line with triangle marker denote the results of simultaneous, 2-Step and 3-Step methods, respectively. As it is shown in Fig. 2(a), all the proposed methods can find the unknown $\mathbf{X}$, $\mathbf{Y}$ and $\mathbf{Z}$ under different noise levels, however, the proposed simultaneous method shows greater performance than the non-simultaneous ones especially in the high noise level. In Fig. 2(b), three methods show similar performances for solving $\mathbf{X}$ and $\mathbf{Z}$, however, the simultaneous method shows greater improvement for $\mathbf{Y}$ in terms of less rotational and translational errors in all noise levels. Additionally, in both Fig. 2(a) and 2(b) the simultaneous method shows more stable solutions than the other two as the errors change smoothly as the number of the data sets increases.

IV. DISCUSSION

The aforementioned results clearly demonstrated that all the simultaneous method and non-simultaneous methods can find hand-eye, tool-flange and robot-robot relationships in different ways with different errors. The superiority of the proposed simultaneous method over the other methods will be compared and discussed from the perspectives listed below.

A. Accuracy and Robustness

Generally, the simultaneous method achieves better accuracy and robustness than non-simultaneous methods, as shown in Fig. 2. For the solutions of $\mathbf{X}$ and $\mathbf{Z}$, the results of simultaneous method are almost as good as the other two, with some exceptions in solving the translation of $\mathbf{Z}$ and some situations with fewer data. However, it is especially significant that the simultaneous method show better results in the solution of $\mathbf{Y}$, which is the transformation between the base frames of the two mobile robots.

A feasible explanation for these results is that the simultaneous method makes a better trade-off to balance the errors within the three unknowns. The non-simultaneous methods solve the unknowns one by one, which leads to the error propagation and accumulation. This is obviously shown by the poor performance of 2-Step and 3-Step solutions of $\mathbf{Y}$. By contrast, the simultaneous one improves the overall accuracy and robustness from a global perspective, it significantly improves the accuracy of $\mathbf{Y}$ with only a little sacrifice of the accuracy of $\mathbf{X}$ and $\mathbf{Z}$. In addition, the simultaneous method shows more stable solutions against higher level of noise.

B. Efficiency In Practice

The simultaneous method is more efficient than the other two when we are about to solve the real problems in practice. First, it is cumbersome or even impossible to obtain data which non-simultaneous methods need. As it is stated in Section II, the data collection processes of the non-simultaneous methods are more complex and thus time-consuming. Additionally, timing sequence issues have to be carefully handled in practice. Second, more measurement data are required when using the non-simultaneous methods in order to achieve the same accuracy as the simultaneous method. This becomes a critical issue when the real-time applications are to be considered.

V. CONCLUSION

We have proposed a simultaneous hand-eye, tool-flange and robot-robot calibration method which is an essential matter for the application of multiple robot cooperation. The problem is formulated as solving a matrix equation $\mathbf{AXB} = \mathbf{YCZ}$. A linear approximation iterative algorithm is put forward, which can efficiently and accurately converge to the true solution given a good initial estimation. Intensive simulations are carried out to demonstrate the superiority of the proposed simultaneous method over non-simultaneous ones in terms of average accuracy and stability against noise.

In our future work, the method of finding an approximate initial point for our iterative algorithm will be investigated in case the hand-eye or tool-flange relationship is difficult to estimate in advance. Solvability analysis of the proposed algorithm will also be explored. In addition, experiments on real robots will be performed to validate the efficiency and robustness of the proposed method.

ACKNOWLEDGMENT

This work is in-part supported by RGC GRF # 415512 awarded to Max Q.-H. Meng, Singapore Academic Research Fund under Grants R397000139133 and R397000157112 awarded to Hongliang Ren. Jiaole Wang would like to acknowledge the Global Scholarship Programme for Research Excellence (CUHK) during 2013-14 to carry out study at the National University of Singapore.

REFERENCES

[1] O. Khatib, K. Yokoi, K. Chang, D. Ruspini, R. Holmberg, and A. Casal, "Vehicle/arm coordination and multiple mobile manipulator decentralized cooperation," in *Proceedings of IEEE/RSJ International Conference on Intelligent Robots and Systems*, vol. 2, 1996, pp. 546–553.

[2] J. S. Mehling, P. Strawser, L. Bridgwater, W. Verdeyen, and R. Rovekamp, "Centaur: Nasa's mobile humanoid designed for field work," in *Proceedings of IEEE International Conference on Robotics and Automation*, 2007, pp. 2928–2933.

[3] A. C. Lehman, K. A. Berg, J. Dumpert, N. A. Wood, A. Q. Visty, M. E. Rentschler, S. R. Platt, S. M. Farritor, and D. Oleynikov, "Surgery with cooperative robots," *Computer Aided Surgery*, vol. 13, no. 2, pp. 95–105, 2008.

[4] H. Ren, C. M. Lim, J. Wang, W. Liu, S. Song, Z. Li, G. Herbert, H. Yu, Z. Tse, and Z. Tan, "Computer assisted transoral surgery with flexible robotics and navigation technologies: A review of recent progress and research challenges," *Critical Reviews in Biomedical Engineering, in press*, 2014.

[5] J. Wang, H. Ren, and M. Meng, "A preliminary study on surgical instrument tracking base on multiple modules of monocular pose estimation," in *CYBER 2014, IEEE International Conference on CYBER Technology in Automation, Control, and Intelligent Systems*. IEEE, 2014, pp. –.

[6] T. Fisher, A. Hamed, P. Vartholomeos, K. Masamune, G. Tang, H. Ren, and Z. T. H. Tse, "Intraoperative magnetic resonance imagingconditional robotic devices for therapy and diagnosis," *Proceedings of the Institution of Mechanical Engineers, Part H: Journal of Engineering in Medicine*, 2014.

[7] H. Ren, W. Liu, and A. Lim, "Marker-based instrument tracking using dual kinect sensors for navigated surgery," *IEEE Transactions on Automation Science and Engineering, in press*, vol. PP, no. 99, pp. 1–4, 2013.

[8] Y. Zhou, H. Ren, M. Q.-H. Meng, Z. T. H. Tse, and H. Yu, "Robotics in natural orifice transluminal endoscopic surgery," *Journal of Mechanics in Medicine and Biology*, vol. 13, no. 02, p. 1350044, 2013.

[9] J. Stoll, H. Ren, and P. E. Dupont, "Passive markers for tracking surgical instruments in real-time 3d ultrasound imaging," *IEEE Transactions on Medical Imaging*, vol. 31, no. 3, pp. 563–575, 2012.

[10] H. Ren and P. Kazanzides, "Investigation of attitude tracking using an integrated inertial and magnetic navigation system for hand-held surgical instruments," *IEEE/ASME Transactions on Mechatronics*, vol. 17, no. 2, pp. 210 –217, 2012.

[11] H. Ren, D. Rank, M. Merdes, J. Stallkamp, and P. Kazanzides, "Multi-sensor data fusion in an integrated tracking system for endoscopic surgery," *IEEE Transactions on Information Technology in Biomedicine*, vol. 16, no. 1, pp. 106 – 111, 2012.

[12] C. Nadeau, H. Ren, A. Krupa, and P. E. Dupont, "Intensity-based visual servoing for instrument and tissue tracking in 3d ultrasound volumes," *IEEE Transactions on Automation Science and Engineering, to appear*, 2014.

[13] K. Wu, F. K. L. Wong, S. J. K. Ng, S. T. Quek, B. Zhou, D. Murphy, Z. J. Daruwalla, and H. Ren, "Statistical atlas-based morphological variation analysis of the asian humerus: Towards consistent allometric implant positioning," *International Journal of Computer Assisted Radiology and Surgery, to appear*, pp. 1–11, 2014.

[14] H. Ren, E. Campos-Nanez, Z. Yaniv, F. Banovac, N. Hata, and K. Cleary, "Treatment planning and image guidance for radiofrequency ablation of large tumors," *IEEE Transactions on Information Technology in Biomedicine (IEEE Journal of Biomedical and Health Informatics)*, vol. 18, no. 3, pp. 920–928, May 2014.

[15] S. Song, H. Ren, and H. Yu, "An improved magnetic tracking method using rotating uniaxial coil with sparse points and closed form analytic solution," *IEEE Sensors Journal, to appear*, 2014.

[16] J. Wang, H. Ren, and M. Meng, "Towards occlusion-free surgical instrument tracking: A multiple monocular modules approach & an agile calibration method," *IEEE Transactions on Automation Science and Engineering, in press*, vol. PP, no. 99, pp. 1–4, 2014.

[17] Y. C. Shiu and S. Ahmad, "Calibration of wrist-mounted robotic sensors by solving homogeneous transform equations of the form $AX = XB$," *IEEE Transactions on Robotics and Automation*, vol. 5, no. 1, pp. 16–29, 1989.

[18] R. Y. Tsai and R. K. Lenz, "A new technique for fully autonomous and efficient 3D robotics hand/eye calibration," *IEEE Transactions on Robotics and Automation*, vol. 5, no. 3, pp. 345–358, 1989.

[19] K. Daniilidis, "Hand-eye calibration using dual quaternions," *The International Journal of Robotics Research*, vol. 18, no. 3, pp. 286–298, 1999.

[20] F. C. Park and B. J. Martin, "Robot sensor calibration: solving $AX = XB$ on the euclidean group," *IEEE Transactions on Robotics and Automation*, vol. 10, no. 5, pp. 717–721, 1994.

[21] K. H. Strobl and G. Hirzinger, "Optimal hand-eye calibration," in *Proceedings of IEEE/RSJ International Conference on Intelligent Robots and Systems*, 2006, pp. 4647–4653.

[22] I. Fassi and G. Legnani, "Hand to sensor calibration: A geometrical interpretation of the matrix equation $AX = XB$," *Journal of Robotic Systems*, vol. 22, no. 9, pp. 497–506, 2005.

[23] A. Malti and J. P. Barreto, "Robust hand-eye calibration for computer aided medical endoscopy," in *Proceedings of IEEE International Conference on Robotics and Automation*, 2010, pp. 5543–5549.

[24] Z. Zhao, "Hand-eye calibration using convex optimization," in *Proceedings of IEEE International Conference on Robotics and Automation*, 2011, pp. 2947–2952.

[25] H. Zhuang, Z. S. Roth, and R. Sudhakar, "Simultaneous robot/world and tool/flange calibration by solving homogeneous transformation equations of the form $AX = YB$," *IEEE Transactions on Robotics and Automation*, vol. 10, no. 4, pp. 549–554, 1994.

[26] F. Dornaika and R. Horaud, "Simultaneous robot-world and hand-eye calibration," *IEEE Transactions on Robotics and Automation*, vol. 14, no. 4, pp. 617–622, 1998.

[27] A. Li, L. Wang, and D. Wu, "Simultaneous robot-world and hand-eye calibration using dual-quaternions and kronecker product," *International Journal of the Physical Sciences*, vol. 5, no. 10, pp. 1530–1536, 2010.

[28] H. Ren and P. Kazanzides, "A paired-orientation alignment problem in a hybrid tracking system for computer assisted surgery," *Journal of Intelligent and Robotic Systems*, vol. 63, no. 2, pp. 151–161, 2011.

[29] F. Ernst, L. Richter, L. Matthäus, V. Martens, R. Bruder, A. Schlaefer, and A. Schweikard, "Non-orthogonal tool/flange and robot/world calibration," *The International Journal of Medical Robotics and Computer Assisted Surgery*, vol. 8, no. 4, pp. 407–420, 2012.

[30] N. Trawny, X. S. Zhou, K. Zhou, and S. I. Roumeliotis, "Interrobot transformations in 3-D," *IEEE Transactions on Robotics*, vol. 26, no. 2, pp. 226–243, 2010.

[31] X. S. Zhou and S. I. Roumeliotis, "Determining the robot-to-robot 3D relative pose using combinations of range and bearing measurements: 14 minimal problems and closed-form solutions to three of them," in *Proceedings of IEEE/RSJ International Conference on Intelligent Robots and Systems*, 2010, pp. 2983–2990.

[32] ——, "Determining 3-D relative transformations for any combination of range and bearing measurements," *IEEE Transactions on Robotics*, vol. 29, no. 2, pp. 458–474, 2013.

[33] J. Selig, *Geometric Fundamentals of Robotics*. New York: Springer-Verlag, 2005.

[34] P. Corke, "Robot arm kinematics," in *Robotics, Vision and Control*. Springer, 2011, pp. 137–170.